04

Using an energy approach to evaluate the parameters of a resonant microwave plasma channel

© V.G. Brovkin, P.V. Vedenin

Joint Institute for High Temperatures, Russian Academy of Sciences,
Moscow, Russia
e-mail: brovkin47@mail.ru

Received July 25, 2025
Revised October 24, 2025
Accepted October 24, 2025

Using numerical simulation, we tested and confirmed the hypothesis that, over a wide range of microwave discharge parameters, a thin plasma filament developing along an electric field in free space tends to absorb maximum energy. Analytical expressions were obtained for the main characteristics (plasma electron conductivity and concentration, electric field in the central region, absorbed power, etc.) of the plasma channel at the „maximum" trajectory, allowing us to estimate the parameters of the formed channel. A comparison with existing experimental data was made.

Keywords: Maxwell's equations, absorbed energy, resonance, plasma channel conductivity, plasmoid dipole moment.

DOI: 10.61011/TP.2026.03.63158.199-25

Introduction

A single free localized microwave thin plasma filament channel (plasmoid) is the object of the study, results of which are described in this work. Plasma channel is interesting for research both from fundamental and applied standpoints. First, at present the fundamental principles of plasma channel self-organization have not been established yet. Second, importance of the investigation of microwave thin plasma filament properties is proved, for example, by an interest in plasma aerodynamics (remote hot channel action on a high-velocity gas flow [1,2]) and in plasma-assisted combustion applications (using the channels for methane/air mixture ignition [3]).

Channels are generally formed in focus of an electromagnetic wave beam(s) far from surfaces in dense gas at $\nu \gg \omega$ (ν is the transport frequency of electron-molecule collisions, and ω is the angular frequency of electromagnetic field oscillations). Longitudinal dimension of a filament that can be seen in photographs (along an external linearly polarized electric field) is generally within $(0.5-0.8)\lambda$ (λ is the incident electromagnetic radiation wavelength), and its typical maximum transverse scale is much smaller than the wavelength.

Findings of a detailed experimental and theoretical investigation of evolution of a free localized microwave plasma channel are described in [4–7 and 7–15], respectively.

Plasmoid develops from an initial plasma cloud in two opposite directions along the external electric field via a streamer mechanism (two scattered ionization waves). As the channel length and conductivity increase, the effect of a vortex electric field becomes increasingly noticeable and prevents extension due to electric field amplitude reduction on the heads. The channel shape during elongation approaches an ellipsoid. At the final stage, the space charge on the heads within the above-mentioned longitudinal dimension range cannot provide further propagation of ionization waves any longer. Recombination restricts the growth of conductivity, while ionization-recombination quasi-equilibrium is approached gradually from the center to ends in a generally already formed plasmoid. After completion of elongation, plasma component concentrations and electric field amplitude are still „breathing" due to their mutual influence via process constants. Later at a gas dynamic stage after a time of about r_{ch}/C_s (r_{ch} is a typical transverse dimension of the channel, C_s is the speed of sound), gas heating leads to gas rarefaction, causing ionization-overheating instability. As a result, a brightly shining cord(s) appears in the central region and has(have) a radius much smaller than transverse dimensions of an enveloping plasmoid [1,4].

As information was accumulated, some typical features of channel evolution at various stages were noted. Thus, for example, within an electrostatic limit, where the role of vortex currents is negligibly low, sizes and conductivity are rising self-consistently so that the field amplitude in the central region varies insignificantly. This is proved by numerical simulation results [7,11,12]. Paper [7] has identified a chain of links between the channel parameters, which is responsible for such amplitude behavior at this stage, however, the cause behind this self-organization mechanism has not been revealed.

A hypothesis that a free localized microwave plasma channel develops in such a way that the absorbed power is as high as possible at any time was suggested in [16,17] and verified in a limited pressure range of $30-100$ Torr. It

should be emphasized that the maximum absorbed power depends only on dimensions of a plasma formation and on plasma space distribution times. Physical content of this hypothesis is as follows: as plasma conductivity grows, electric field amplitude in the internal region decreases. Therefore, there are conditions, at which the plasma-absorbed power is as high as possible. We believe that the foregoing is also applicable to a wider class of discharges. Self-organization mechanisms inducing the maximum power absorption are studied in [18].

This work was focused on an application aspect of the microwave channel evolution study. The purpose of the study was to obtain universal relations that allowed the main properties of the formed quasistatic plasma formation to be evaluated on the basis of the above-mentioned hypothesis and experimental data concerning the visible dimensions of this formation.

1. Interaction between microwave radiation and thin plasma channel

A thin plasma channel evolves in an electric field of a linearly polarized electromagnetic wave. $\mathrm{Re}[\mathbf{E}_0(\mathbf{r})\exp(-i\omega t + i\mathbf{kr})]$. The visible longitudinal dimension of the channel $2Z_{vis}$ (along the external electric field) is limited by $2Z_{vis} < \lambda$, and its visible transverse dimensions $2X_{vis}$, $2Y_{vis}$ are much smaller than the wavelength. Plasma is quasineutral. Electrons oscillate relative to the ion background that is static for the oscillation period T ($T = 2\pi/\omega$). Variations of plasma cloud dimensions and plasma concentration are negligibly small for the electromagnetic field oscillation period. High-frequency oscillations cause uncompensated high-frequency space charges of opposite signs $\pm|\rho_e^h|$ that are positioned symmetrically about the center of the channel and localized predominantly at the filament ends in the maximum conductivity gradient regions. This follows from

$$\rho_e^h = -\frac{i\nabla\cdot\mathbf{j}_e^h}{\omega} = -\varepsilon_0\mathbf{E}\nabla\varepsilon \propto \nabla N_e, \tag{1}$$

where $\mathbf{j}_e^h$ is the density of electron current induced by the external electric field ($\mathbf{j}_e^h = \sigma\mathbf{E}/(1 - j\vartheta)$), $\sigma = e^2N_e/m\nu$ is the plasma electron conductivity, $N_e(\mathbf{r}, t)$ is the concentration of plasma electrons averaged over the electromagnetic field oscillation period; $\vartheta = \omega/\nu$ ($\vartheta = \mathrm{const}$ at the „fast“ channel elongation stage as discussed in this work), $\varepsilon = 1 + i\sigma_*/(1 - i\vartheta)$ is the complex permittivity of plasma, $\sigma_* = \sigma/\omega\varepsilon_0$, ε_0 is the permittivity of vacuum.

Formal solution of the Maxwell equations for slowly varying complex amplitudes of the high-frequency electric field in case of interaction between the field and the thin plasma filament can be conveniently written in the following integral form:

$$\mathbf{E}(\mathbf{r}, t) = \mathbf{E}_0(\mathbf{r})\exp(i\mathbf{kr}) + \mathbf{E}_p(\mathbf{r}, t), \tag{2}$$

where $\mathbf{E}_p = \mathbf{E}_\rho + \mathbf{E}_j$ is the plasma response field, $\mathbf{E}_\rho$, $\mathbf{E}_j$ are the fields generated by high-frequency chargers

$$\mathbf{E}_\rho(\mathbf{r}, t) = -\frac{k}{4\pi\varepsilon_0}\int dV' G(\kappa)\nabla'\rho_e^h(\mathbf{r}', t),$$

and current

$$\mathbf{E}_j(\mathbf{r}, t) = \frac{i\omega\mu_0 k}{4\pi}\int dV' G(\kappa)\mathbf{j}_e^h(\mathbf{r}', t),$$

μ_0 is the free space permeability, $G = \exp(i\kappa)/\kappa$ is Green's function. Here, $\kappa = k|\mathbf{r} - \mathbf{r}'|$.

Expression for high-frequency field amplitude in the central region of the channel, where almost all plasma is concentrated, is written as [6]:

$$E_c \approx \frac{E_0}{1 + i\frac{\sigma_{*c}\Psi_c}{1 - i\vartheta}}, \tag{3a}$$

where

$$\Psi_c = -\frac{k^3}{4\pi}\int dV f(\mathbf{r}, t)G(\kappa_c)\Big[1 + i\kappa_c^{-1} - \kappa_c^{-2} - \xi_{zc}^2(1 + 3i\kappa_c^{-1} - 3\kappa_c^{-2})\Big], \tag{3b}$$

$f(\mathbf{r}) = \sigma(\mathbf{r})/\sigma_c$, $\xi_{zc} = z/r$, $\kappa_c = kr$, $r = \sqrt{x^2 + y^2 + z^2}$.

It should be emphasized that the electric field in the center depends integrally on the plasma conductivity distribution. Integral dependence means that consideration of the details of this distribution cannot cause a noticeable influence on the amplitude.

Expression (3b) for a filament with a smaller wavelength can be transformed as follows:

$$\Psi_c = n_z - k^2X_{vis}Y_{vis}\sum_{m=0}\frac{(ikZ_{vis})^m\psi_m}{m!(m+2)}, \tag{3c}$$

$$n_z \equiv \frac{X_{vis}Y_{vis}}{Z_{vis}^2}n_{z*},\ n_* = \frac{1}{4\pi}\int dV_*\left(-\frac{\partial f}{\partial z_*}\right)\frac{z_*}{R_*^3},$$

$$R_* = \sqrt{\left(\frac{x_*}{h_x}\right)^2 + \left(\frac{y_*}{h_y}\right)^2 + z_*^2},$$

$$x_*, y_*, z_* = x/X_{vis}, y/Y_{vis}, z/Z_{vis}$$

$$h_{x,y} = Z_{vis}/X_{vis}, Y_{vis},$$

$$\psi_m = \frac{1}{4\pi}\int dV_* f\Big[(m+1)R_*^{m-1} - (m-1)z_*^2R_*^{m-3}\Big].$$

It should be noted that

$$n_{z*} \approx \begin{cases}\frac{1}{2}, & \text{homogeneous cylinder,}\\ \ln\frac{2Z_{vis}}{R_{vis}}, & \text{ellipsoid of revolution.}\end{cases} \tag{4}$$

2. Analysis of plasma channel evolution within the maximum energy absorption hypothesis

Approximated expression for total absorbed power in the thin plasma channel averaged over a period is written as [16]:

$$W_J \approx \frac{|E_c|^2 \int dV \mathrm{Re}\,\sigma^h}{2} = kS_0 V_{\mathrm{eff}} \frac{\sigma_{*c}}{(1-\sigma_{*c}\mathrm{Im}\Psi_c)^2 + (\sigma_{*c}\mathrm{Re}\Psi_c - \vartheta)^2}, \quad (5)$$

where $S_0 = cE_0^2\varepsilon_0/2$, $V_{\mathrm{eff}} = \int dV f$ is the effective volume. $\mathrm{WJ}[\sigma_{*c}(t)]$ has its maximum because the electric field amplitude in the channel decreases as the conductivity grows. At the normalized conductivity

$$\sigma_{*c}^{(m)}(t) = \frac{\sqrt{1+\vartheta^2}}{|\Psi_c(t)|} \quad (6)$$

the total absorbed power is as high as possible: where

$$W_{res} = \frac{3\lambda^2 S_0}{4\pi\left(1+\sqrt{1+\vartheta^2}\right)}, \quad (8)$$

$$\begin{pmatrix}\chi\\ \mu\end{pmatrix} = \mp \frac{3}{k^3 X_{vis} Y_{vis} Z_{vis}\psi_1} \begin{pmatrix}\mathrm{Im}\\ \mathrm{Re}\end{pmatrix} \Psi_c = \begin{pmatrix} 1 \\ \frac{3}{(kZ_{vis})^3\psi_1}\left(n_* - \frac{(kZ_{vis})^2\psi_0}{2}\right)\end{pmatrix} \pm \sum_{m=1}^{\infty}(-1)^{m+1}\begin{pmatrix}\delta_{2m+1}\\ \delta_{2m}\end{pmatrix},\ \delta_m = \frac{3(kZ_{vis})^{m-1}\psi_m}{m!(m+2)\psi_1}.$$

Equation (8) in air transforms into

$$W_{res}^{(air)} = \frac{1+\vartheta^2}{1+\sqrt{1+\vartheta^2}}\left(P[\mathrm{Torr}]\lambda[\mathrm{cm}]\frac{E_0}{E_{br}}\right)^2,\ [\mathrm{W}], \quad (8a)$$

where E_{br} is the breakdown field, $E_{br}/P = 40\mathrm{V}\cdot\mathrm{cm}^{-1}\cdot\mathrm{Torr}^{-1}$.

Power density in the center is related to the total absorbed power as follows

$$W_{Jc\,\max} \approx \frac{W_{J\max}}{V_{\mathrm{eff}}}. \quad (9)$$

Expression for the field amplitude in the center in the maximum power absorption trajectory is written as

$$\left|E_c^{(m)}\left[\sigma_{*c}^{(m)}(t)\right]\right| \approx \frac{E_0}{\sqrt{2}}\left[1 - \frac{\vartheta\mu - \chi}{\sqrt{(1+\vartheta^2)(\mu^2+\chi^2)}}\right]^{-\frac{1}{2}}. \quad (10)$$

Using expressions (6)–(10), microwave channel evolution in an extreme trajectory is analyzed at a qualitative level.

At the stage of electron avalanche propagation in the incident electric field, the absorbed power is close to zero. At the beginning of elongation in the electrostatic limit ($2Z_{vis} < 0.3\lambda$, $\mu(Z_{viz}) \gg 1$), the above-mentioned properties vary as follows:

$$\sigma_{*c}^{(m)}(t) = \frac{\sqrt{1+\vartheta^2}}{n_z} = \frac{Z_{viz}^2\sqrt{1+\vartheta^2}}{X_{viz}Y_{viz}n_{z*}}, \quad (11)$$

$$W_{J\max} \approx \frac{kS_0 V_{\mathrm{eff}}}{4n_z\left(\sqrt{1+\vartheta^2}-\vartheta\right)} \propto \frac{Z_{viz}^3\eta\xi}{n_{z*}}, \quad (12)$$

$$W_{Jc\,\max} \approx \frac{kS_0}{4n_z\left(\sqrt{1+\vartheta^2}-\vartheta\right)} \propto \frac{Z_{viz}^2}{X_{viz}Y_{viz}n_{z*}}, \quad (13)$$

where

$$\eta = \frac{V_{\mathrm{eff}}}{V_{vis}},\ \xi = \frac{V_{vis}}{2\pi X_{vis}Y_{vis}Z_{vis}}.$$

Since almost all plasma is localized in the volume that can be seen in photographs [7,17], the plasma channel characteristic η reflects a degree of occupation of this volume by plasma, and the geometric factor ξ is evaluated on the basis of the channel shape data. Thus, for example, $\xi = 1;\ 2/3$ for a cylinder and ellipsoid of revolution, respectively. Electric field amplitude at the electrostatic stage of microwave streamer propagation in the central region is close to a constant value

$$\left|E_c^{(m)}\left[\sigma_{*c}^{(m)}(t)\right]\right| \approx \frac{E_0}{\sqrt{2}}\left(1+\frac{\vartheta}{2}\right), \quad (14)$$

which is independent on the computational geometry selection (2*D*-planar or 2*D*-azimuthally symmetric), plasma region shape, etc. This conclusion, as mentioned in the introduction, corresponds to the numerical simulation data.

As the channel length grows, the effect of the vortex electric field becomes increasingly noticeable, therefore $\mu(Z_{viz})$ decreases, and after transition to the resonance region $\mu(Z_{viz}) < 1$, the rate of power rise $w_{Jc\,\max}(Z_{viz})$, $W_{J\max}(Z_{viz})$ rapidly drops. The absorbed power approaches the maximum value. It should be mentioned that in this range of the typical scale Z_{viz}, $\chi(Z_{viz}) \approx 1$.

3. Resonance

For further analysis, expressions for form-factors ψ_m shall be simplified, i.e. spatial distribution of conductivity shall be specified. Results of experiments [4–7,19,20] have shown that the plasma channel has a shape close to an ellipse with the transverse scales X_{viz} and Y_{viz}. Relation of these scales depends on the spatial distribution of the external electric field amplitude near the electrodynamic system focus. In experiments described in [6,7,19,20], channels with $X_{viz} \approx Y_{viz}$ were ignited. In [6], it is shown that when

$$Z_{viz} \geq 4Y_{viz},\ X_{viz} < Y_{viz} \leq 2X_{viz}$$

are satisfied, estimates can use an approximation of ellipsoid of revolution with the averaged radius

$$\overline{R}_{viz} = \sqrt{0.5\left(X_{viz}^2 + Y_{viz}^2\right)}.$$

This result allows the conductivity distribution to be approximated as follows:

$$\sigma(\mathbf{r}, t) = \sigma_c(t) f(t, \xi), \qquad (15)$$

where $\xi = \sqrt{\left(r/\overline{R}_{viz}\right)^2 + \left(z/Z_{viz}\right)^2}$, f is the function meeting $f(\xi = 0) = 1$, $f(\xi \to \infty) \to 0$. Expressions for form-factors were derived in [17] and are written as

$$n_{z*} \approx \ln(2H_{vis}) - 1,$$

$$\psi_0 \approx \gamma_0(2\ln(2H_{vis}) - 1)(\overline{R}_{viz} \ll Z_{vis}),$$

$$\delta_m = \frac{3(kZ_{vis})^{(m-1)}\gamma_m}{m!\, m(m+2)\gamma_1}, \quad \gamma_m = \int d\xi \xi^{m+1} f(\xi),$$

$$H_{vis} = Z_{vis}/\overline{R}_{viz}.$$

According to the experiment, the highest glow intensity is in the central region. This fact suggests that almost all plasma is localized in the luminous region $\xi \leq 1$. For the conductivity distribution with its maximum in the center of plasmoid, it is apparent that $\gamma_{m\geq 2}/\gamma_1 < 1$. Therefore, in the $2Z_{vis} \geq 0.7\lambda$ region of interest, corrections δ_2 and δ_3 are small.

Near the resonance $|\mu(Z_{vis})| \ll 1$, $\chi(Z_{vis}) \approx 1$, expression (7) is extremely simplified and becomes as follows

$$W_{J\max} \approx W_{res}\left(1 + \delta_3 + \frac{\mu(2\vartheta - \mu)}{4}\right). \qquad (16)$$

The absorbed power maximum is reached near $\mu(Z_{viz}) \approx \vartheta$. In view of the foregoing, it is concluded that

$$W_{J\max}^{(res)} \approx W_{res}\left(1 + \delta_3 + \frac{\vartheta^2}{4}\right) \approx W_{res}. \qquad (17)$$

The total absorbed power of the resonance plasmoid explicitly doesn't depend on the transverse scales, and its magnitude is weakly affected by only the conductivity distribution profile via γ_3/γ_1 ($\delta_3 \propto \gamma_3/\gamma_1$) and ϑ.

The figure shows the relative deviation$W_{J*} - 1$ ($W_{J*} = W_{J\,calc}/W_{res}$) of the calculated total absorbed power $W_{J\,calc}$ in resonance vs. normalized plasmoid resonance length $2Z_{res}/\lambda$ for $\lambda = 2$; 12 cm in the range of discharge parameters in air $P = 30{-}750$ Torr, $E_{\text{eff}} = (1.1{-}1.5)E_{br}$. The figure proves that estimate (17) is true and establishes the visible resonance plasmoid length range. The average value of this scale is approximately equal to 0.68λ.

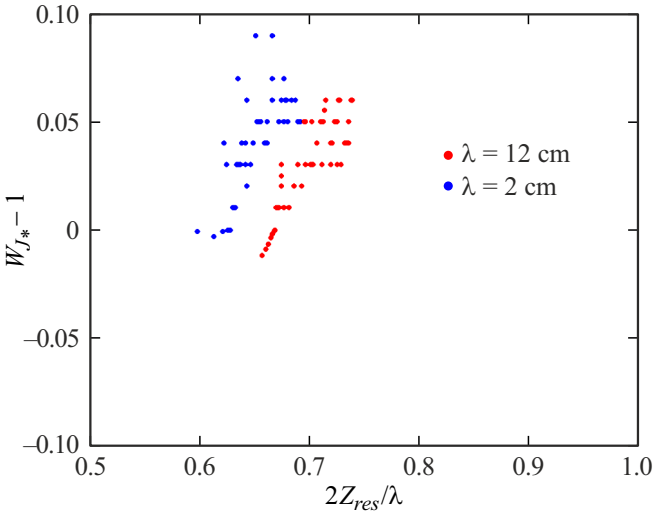

Relative deviation $W_{J*} - 1$ of the calculated total absorbed power $W_{J\,calc}$ in resonance vs. normalized plasmoid resonance length $2Z_{res}/\lambda$ for $\lambda = 2$; 12 cm in the range of discharge parameters in air $P = 30{-}750$ Torr, $E_{\text{eff}} = (1.1{-}1.5)E_{br}$.

4. Parameters of the resonance microwave plasma channel

After reaching the absolute maximum, $W_{J*}(2Z_{vis}/\lambda)$ weakly damps out and oscillates near 1. Plasmoid elongation almost stops. With $Z_{viz} \approx \text{const}$ ($2Z_{viz} > 0.7\lambda$), damped oscillations are the response of ψ_m to conductivity profile deformation, which continues weakly varying near the ionization-recombination quasi-equilibrium state. At this stage, the role of diffusion in the regions of maximum conductivity gradients at the plasmoid ends grows significantly. Analysis of the photographs made at $P = 30 - 150$ Torr suggested that very thin sparks were „shot" occasionally from the heads, decaying afterwards without leading to any significant outcomes.

Plasmoid accumulates energy at the final quasi-steady-state stage of evolution ($t > t_{qs}$, t_{qs} -is the time of approaching this stage), when its sizes and plasma conductivity in the central region are close to limits. t_{qs} can be found experimentally from the analysis of scattered radiation and PMT waveforms (signal behavior characteristics are analyzed in detail in [6]). Thus, for rough upper-bound estimate of energy absorbed during the pulse time, the following equation can be used:

$$Q_{J\max} \approx W_{res}(t_p - t_{qs}). \qquad (18)$$

Relative deviations of channel characteristics

$$\Delta_{E,W,\sigma} \equiv 1 - \frac{|E_c|}{|E_c^{(m)}|}, \quad \frac{W_J}{W_{J\max}}, \quad \frac{\sigma_c}{\sigma_c^{(m)}}$$

from their values in the extreme trajectory are related as

$$\Delta_\sigma \approx 2\sqrt{\Delta_W}, \quad \Delta_E \approx -\sqrt{\Delta_W}, \qquad (19)$$

from which it follows that

$$|\Delta_\sigma|,\ |\Delta_E| \ll 1, \tag{20}$$

if $\Delta_W \ll 1$. Relying on the finding $\Delta_W \ll 1$ and using relations (19), the electric field amplitude and conductivity in the center of the resonance plasmoid can be estimated.

Expression (10) for the electric field amplitude transforms as follows:

$$\left|E_{c\,res}^{(m)}\right| \approx \frac{E_0}{2} + O(\vartheta^2). \tag{21}$$

Conductivity and specific absorbed power in center of plasmoid are inversely proportional to the effective volume

$$V_{\text{eff}} \approx \eta\,\frac{4\pi\overline{R}_{viz}^2 Z_{viz}}{3}. \tag{22}$$

It should be recalled that η reflects the degree of occupation of this volume by plasma. If the visible volume can be estimated using photographs, then the degree of occupation by plasma is determined via numerical calculations. The calculations have shown that the average value in resonance is $\overline{\eta}_{calc} \approx 0.33$, and the maximum deviation from the average value is approximately 20 %.

Expression for conductivity can be conveniently written as

$$\sigma_{c\,res} = \frac{\sigma_{*c\,res}}{60\lambda[\text{cm}]},\ \Omega^{-1}\cdot\text{cm}^{-1},\ \sigma_{*c\,res} = \frac{9H_{vis}^2\sqrt{1+\vartheta^2}}{2\overline{\eta}_{calc}(\pi L_*)^3}. \tag{23}$$

where $L_* = 2Z_{vis}/\lambda$.

In air with $P[\text{Torr}]\lambda[\text{cm}] > 12\pi$ ($\vartheta^2 \ll 1$), we have

$$\sigma_{ec\,res}^{(air)} = \frac{3}{40\lambda[\text{cm}]}\,\frac{H_{vis}^2}{\overline{\eta}_{calc}(\pi L_*)^3} + O(\vartheta^2),\ [\Omega^{-1}\cdot\text{cm}^{-1}]. \tag{24}$$

$$N_{ec\,res}^{(air)} \approx \frac{4.8\cdot 10^{10}P[\text{Torr}]H_{vis}^2}{\overline{\eta}_{calc}\lambda[\text{cm}]L_*^3} + O(\vartheta^2),\ [\text{cm}^{-3}]. \tag{25}$$

Here, for effective frequency of electron-molecule collisions, approximation $\nu \approx 5\cdot 10^9 P[\text{Torr}]$, s^{-1} was used.

Using equation (25) and experimental data on visible dimensions, electron concentration in the centers of channels described in [6,19,20] was estimated. The results are shown in the table. Note that papers [6,19] studied the discharge in sufficiently wide air pressure ranges ($P = 30 - 150$ Torr [6], $P = 50-100$ Torr [19]), however, the visible plasmoid dimensions varied insignificantly. Therefore, the scales listed in the table can be used to estimate the electron concentration at other pressures.

Dipole moment of plasma channel is the main property that defines the channel's capability to scatter electromagnetic waves. Information about the magnitude of dipole moment is used for evaluation of integral parameters of the plasma formation (inverse scattering problem). In the case of interaction between a thin plasmoid and electromagnetic radiation, an expression for longitudinal (along the external electric field) component of the dipole moment is written as

Estimated electron concentrations in the centers of plasmoids

λ, cm	P, Torr	Z_{vis}, cm	$X_{vis} \approx Y_{vis}$, cm	$\hat{N}_{ec}^{(air)}$, cm^{-3}
2.3 [6]	75	0.8	0.13	$5\cdot 10^{14}$
3 [19]	75	1	0.3	$1.4\cdot 10^{14}$
8.5 [20]	750	1.7	0.2	$1.5\cdot 10^{16}$

$$d_z \approx \frac{i\sigma_c E_c V_{\text{eff}}}{(1-i\vartheta)\omega}. \tag{26}$$

Experimental study [6] has shown that the normalized dipole moment amplitude $d_* = k^3 d_z/4\pi\varepsilon_0 E_0$ is virtually independent of air pressure, ranging between 0.5–0.7.

Substitution of expressions (6) into expression (26) establishes the following relation between the normalized dipole moment and electric field amplitudes in the maximum trajectory:

$$\left|d_*^{(m)}\right| \approx 1.5\frac{\left|E_c^{(m)}\right|}{E_0\sqrt{\mu^2+\chi^2}}. \tag{27}$$

Consequently, in resonance we have

$$\left|d_{*\,res}\right| \approx 0.75 + O(\vartheta^2). \tag{28}$$

The obtained estimate agrees well with the experimental findings and proves the hypothesis of maximum power absorption by a free localized microwave plasma channel during its evolution.

Results

In a wide range of discharge parameters in air $\lambda = 2$; 12 cm, $P = 30-750$ Torr, $E_{\text{eff}} = (1.1-1.5)E_{br}$, the following hypothesis was checked and proved: the microwave thin plasma channel develops in such a way that the power absorbed by the channel at any time is close to the maximum possible value at this time. Evolution of the microwave channel in the extreme trajectory has been analyzed qualitatively.

Information regarding the degree of occupation of a plasma volume visible in photographs by plasma has been obtained to estimate local properties of the channel in the central region.

Universal relations have been derived to establish correlations between the key properties of plasmoid (total and specific absorbed powers, total absorbed energy, electric field amplitude, conductivity and plasma concentration in the central region, dipole moment) and discharge parameters (wavelength, pressure, electric field amplitude), plasmoid dimensions and occupation of the apparent volume by plasma.

The derived equations were used to estimate the electron concentration in the experimentally observed plasma channels.

Universal normalized dipole moment of plasmoid agrees well with the experimental result.

Funding

This study was supported by the Ministry of Science and Higher Education of the Russian Federation (state order No. 075-00269-25-00).

Conflict of interest

The authors declare no conflict of interest.

References

[1] Yu.F. Kolesnichenko, V.G. Brovkin, O.A. Azarova, V.G. Grudnitsky, V.A. Lashkov, I.Ch. Mashek. AIAA, 2003-0361 (2003).
[2] D. Knight. J. Aerospace Lab., **10**, AL10-02 (2015).
[3] J.B. Michael, A. Dogariu, M.N. Shneider, R.B. Miles. J. Appl. Phys., **108**, 093308 (2010).
[4] A.L. Vikharev, A.M. Gorbachev, A.V. Kim, A.L. Kolysko. Fizika Plazmy, **18** (8), 1064 (1992) (in Russian).
[5] A.S. Zarin, A.A. Kuzovnikov, V.M. Shibkov. *Svobodno lokalizovanny SVCh razryad v vozdukhe* (Neft i gaz, M., 1996) (in Russian)
[6] V.A. Bityurin, V.G. Brovkin, P.V. Vedenin. J. Phys. D: Appl. Phys., **50**, 275201 (2017).
[7] V.G. Brovkin, P.V. Vedenin. J. Appl. Phys., **128**, 113301 (2020).
[8] V.B. Gildenburg, I.S. Gushchin, S.A. Dvinin. ZhETF, **97** (4), 1151 (1990) (in Russian).
[9] P.V. Vedenin, N.E. Rozanov. ZhETF, **105** (4), 868 (1994) (in Russian).
[10] P.V. Vedenin, N.A. Popov. ZhETF, **108** (2), 531 (1995) (in Russian).
[11] G.V. Naidis. ZhETF, **109** (4), 1288 (1996) (in Russian).
[12] V.A. Bityurin, P.V. Vedenin. ZhETF, **138** (3), 577 (2010) (in Russian).
[13] B. Chaudhury, J.P. Boeuf, G.Q. Zhu, O. Pascal. J. Appl. Phys., **110**, 113306 (2011).
[14] K. Kourtzanidis, J.P. Boeuf, F. Rogier. Phys. Plasmas, **21**, 123513 (2014).
[15] K. Kourtzanidis, F. Rogier, J. Boeuf. J. Appl. Phys., **118**, 103301 (2015).
[16] V.G. Brovkin, P.V. Vedenin, Ch. Mashek. J. Phys.: Conf. Ser., **1698**, 012013 (2020).
[17] V.G. Brovkin, P.V. Vedenin. J. Appl. Phys., **131**, 123302 (2022).
[18] V.G. Brovkin, P.V. Vedenin. Plasma Sources Sci. Technol., **31**, 094007 (2022).
[19] Yu.F. Kolesnichenko, V.G. Brovkin, D.V. Khmara, V.A. Lashkov, I.Ch. Mashek, M.I. Ryvkin. AIAA, 2003-0362 (2003).
[20] L.P. Grachev, I.I. Yesakov, G.I. Mishin, K.V. Khodataev. ZhTF, **64** (2), 26 (1994) (in Russian).

Translated by E.Ilyinskaya